Research Article | Vol. 8, No. 11 | 1 Nov 2017 | BIOMEDICAL OPTICS EXPRESS 4827
Biomedical Optics EXPRESS

Lens internal curvature effects on age-related eye model and lens paradox

STEFANO GIOVANZANA,[1,*] TANYA EVANS,[2] AND BARBARA PIERSCIONEK[3]

[1]*Studio Optometrico Giovanzana, Milano, Italy*
[2]*Department of Optometry, University of Johannesburg, Johannesburg, South Africa*
[3]*College of Science and Technology, School of Science & Technology, Nottingham Trent University, Nottingham, UK*
**s.giovanzana82@gmail.com*

Abstract: The gradient index (GRIN) model is the most accurate way to represent the eye lens which, because of its growth mode, is a lamellar, shell-like structure. The GRIN is thought to provide optical properties that counteract age-related changes in curvature that would otherwise create an increasingly myopic eye: the so-called lens paradox. This article investigates how fine-tuning the refractive index and the internal curvatures of the lenticular indicial contours may prevent the ageing eye from becoming myopic. A system matrix approach is applied for analysis of a shell model with 200 shells to obtain the paraxial characteristics of the eye model.

OCIS codes: (170.4460) Ophthalmic optics and devices; (330.5370) Physiological optics; (330.7323) Visual optics, aging changes; (330.7326) Visual optics, modeling; (110.2760) Gradient-index lenses.

References and links

1. M. Dubbelman, V. A. Sicam, and G. L. Van der Heijde, "The shape of the anterior and posterior surface of the aging human cornea," Vision Res. **46**(6-7), 993–1001 (2006).
2. M. Dubbelman, G. L. van der Heijde, and H. A. Weeber, "The thickness of the aging human lens obtained from corrected Scheimpflug images," Optom. Vis. Sci. **78**(6), 411–416 (2001).
3. M. Dubbelman and G. L. Van der Heijde, "The shape of the aging human lens: Curvature, equivalent refractive index and the lens paradox," Vision Res. **41**(14), 1867–1877 (2001).
4. B. Pierscionek, M. Bahrami, M. Hoshino, K. Uesugi, J. Regini, and N. Yagi, "The eye lens: age-related trends and individual variations in refractive index and shape parameters," Oncotarget **6**(31), 30532–30544 (2015).
5. H. von Helmholtz, *Physiologische Optik*, 3rd ed. (Voss, Hamburg 1909).
6. A. Gullstrand, appendix in *Physiologische Optik*, 3rd ed., H. von Helmholtz, Ed., Voss, Hamburg (1909).
7. H. H. Emsley, *Visual Optics*, 5th ed., Vol. 1, (Hatton Press Ltd., London 1952).
8. Y. Le Grand *Optique Physiologique* I, eds., Rev. Opt., Paris (1953).
9. W. Lotmar, "Theoretical eye model with aspherics," J. Opt. Soc. Am. **61**(11), 1522–1529 (1971).
10. N. Drasdo and C. W. Fowler, "Non-linear projection of the retinal image in a wide-angle schematic eye," Br. J. Ophthalmol. **58**(8), 709–714 (1974).
11. A. C. Kooijman, "Light distribution on the retina of a wide-angle theoretical eye," J. Opt. Soc. Am. **73**(11), 1544–1550 (1983).
12. R. Navarro, J. Santamaría, and J. Bescós, "Accommodation-dependent model of the human eye with aspherics," J. Opt. Soc. Am. A **2**(8), 1273–1281 (1985).
13. H. L. Liou and N. A. Brennan, "Anatomically accurate, finite model eye for optical modeling," J. Opt. Soc. Am. A **14**(8), 1684–1695 (1997).
14. S. Norrby, "The Dubbelman eye model analysed by ray tracing through aspheric surfaces," Ophthalmic Physiol. Opt. **25**(2), 153–161 (2005).
15. A. V. Goncharov and C. Dainty, "Wide-field schematic eye models with gradient-index lens," J. Opt. Soc. Am. A **24**(8), 2157–2174 (2007).
16. N. Brown, "The change in lens curvature with age," Exp. Eye Res. **19**(2), 175–183 (1974).
17. B. Pierscionek, "Presbyopia–effect of refractive index," Clin. Exp. Optom. **73**(1), 23–30 (1990).
18. G. Smith and B. K. Pierscionek, "The optical structure of the lens and its contribution to the refractive status of the eye," Ophthalmic Physiol. Opt. **18**(1), 21–29 (1998).
19. D. A. Atchison, E. L. Markwell, S. Kasthurirangan, J. M. Pope, G. Smith, and P. G. Swann, "Age-related changes in optical and biometric characteristics of emmetropic eyes," J. Vis. **8**(4), 29 (2008).
20. R. Navarro, F. Palos, and L. González, "Adaptive model of the gradient index of the human lens. I. Formulation and model of aging *ex vivo* lenses," J. Opt. Soc. Am. A **24**(8), 2175–2185 (2007).

#302294 https://doi.org/10.1364/BOE.8.004827
Journal © 2017 Received 12 Jul 2017; revised 20 Sep 2017; accepted 25 Sep 2017; published 3 Oct 2017

Biomedical Optics EXPRESS

21. O. Pomerantzeff, M. Pankratov, G. J. Wang, and P. Dufault, "Wide-angle optical model of the eye," Am. J. Optom. Physiol. Opt. **61**(3), 166–176 (1984).
22. C. J. Sheil, *Modelling accommodation and ageing of the crystalline lens in the human eye*, Ph.D. Thesis National University of Ireland, Galway (2016).
23. C. J. Sheil and A. V. Goncharov, "Accommodating volume-constant age-dependent optical (AVOCADO) model of the crystalline GRIN lens," Biomed. Opt. Express **7**(5), 1985–1999 (2016).
24. W. F. Harris, "Magnification, blur, and ray state at the retina for the general eye with and without a general optical instrument in front of it: 1. Distant Objects," Optom. Vis. Sci. **78**(12), 888–900 (2001).
25. T. Evans and W. F. Harris, "Dependence of the transference of a reduced eye on frequency of light," S. Afr. Optom. **70**, 149–155 (2011).
26. C. E. Jones, D. A. Atchison, R. Meder, and J. M. Pope, "Refractive index distribution and optical properties of the isolated human lens measured using magnetic resonance imaging (MRI)," Vision Res. **45**(18), 2352–2366 (2005).
27. R. Navarro and N. Lopez-Gil, "Impact of the internal curvature gradient on the power and accommodation of the crystalline lens," Optica **4**(3), 334–340 (2017).
28. G. Smith, D. A. Atchison, and B. K. Pierscionek, "Modelling the ageing human eye," J. Opt. Soc. Am. A **9**(12), 2111–2117 (1992).
29. B. K. Pierscionek and J. W. Regini, "The gradient index lens of the eye: an opto-biological synchrony," Prog. Retin. Eye Res. **31**(4), 332–349 (2012).
30. D. Lahm, L. K. Lee, and F. A. Bettelheim, "Age dependence of freezable and nonfreezable water content of normal human lenses," Invest. Ophthalmol. Vis. Sci. **26**(8), 1162–1165 (1985).
31. P. R. Eva, P. T. Pascoe, and D. G. Vaughan, "Refractive change in hyperglycaemia: hyperopia, not myopia," Br. J. Ophthalmol. **66**(8), 500–505 (1982).
32. W. N. Charman, Adnan, and D. A. Atchison, "Gradients of refractive index in the crystalline lens and transient changes in refraction among patients with diabetes," Biomed. Opt. Express **3**(12), 3033–3042 (2012).
33. S. F. Lin, P. K. Lin, F. L. Chang, and R. K. Tsai, "Transient hyperopia after intensive treatment of hyperglycemia in newly diagnosed diabetes," Ophthalmologica **223**(1), 68–71 (2009).
34. B. E. Klein, K. E. Lee, and R. Klein, "Refraction in adults with diabetes," Arch. Ophthalmol. **129**(1), 56–62 (2011).

1. Introduction

Ageing manifests in different parts of the eye at varying rates. These include the anterior and posterior asphericities of the cornea [1], the anterior chamber depth [2], and most pertinently, the crystalline lens [3, 4] which changes with age as it grows. Early eye models, such as Helmholtz [5], Gullstrand [6], Emsley [7] and Le Grand [8], used a limited number of spherical surfaces to model the real eye and their purpose is to analyze first-order aberrations. Subsequent models, such as the wide-angle systems of Lotmar [9], Drasdo and Fowler [10], Kooijman [11], Navarro et al. [12], Liou and Brennan [13], Norrby [14] and Goncharov and Dainty [15], introduced aspherical surfaces to provide improved fits to real data as well as for other applications that predict retinal image size [10] or analyze the light level on the retina [11]. Some of these models incorporate a GRIN lens [12, 13, 15], are dependent on accommodation level [12, 14] or on age [14].

The lens thickness, and anterior and posterior lens curvatures increase with age [3]. With no alterations in the refractive index such geometric changes with age would lead to myopia. This has been deemed the lens paradox [16]. A theory was proposed to explain that the refractive index may alter with age to counter any myopic change [17]. This was subsequently supported in a number of models [18–21].

One of the lens models that incorporates shells of varying refractive index was that of Pomerantzeff et al. [21]. In this model the surface of the lens and the nucleus have different curvatures and the surface shape of the lens differs from the biological lens with anterior and posterior surfaces meeting at a point at the equator. Subsequently, Sheil [22] suggested that changing the internal curvatures of GRIN shells can be more effective than altering the GRIN profile when counteracting curvature changes. The links between internal indicial contours and internal surface curvatures are not directly related according to the AVOCADO model [23]. The relationship between curvatures and refractive index contours of the lens requires further analysis.

The present work investigates the paraxial properties of the eye, applying a general approach to different lens models. This method is based on the *ABCD* system matrix [24, 25]

Biomedical Optics EXPRESS

as this allows an analysis of the effects of the internal structures on the entire system. It is shown here that changing the inner curvatures of the indicial contours of the lens can counteract shape changes with age and offset an increase in myopia.

2. Method

2.1 Eye model

An age-related eye model was constructed using parameters and external lens curvatures from the study by Atchison *et al*. [19]. These are given in Table. 1. The ratio between anterior lens thickness and total lens thickness is taken as 0.5399 [4].

Table 1. Data for the eye model.

	Radius (mm)	*n*	Distance (mm)
Ant. Cornea (K1)	7.75		
Cornea (K)		1.376	0.539
Post. Cornea (K2)	6.50		
Ant. Chamber (AC)		1.336	$3.318 - 0.0106 \cdot Age$
Ant. Lens (AL)	$12.283 - 0.0438 \cdot Age$		
Lens (L)		GRIN	$3.1267 + 0.02351 \cdot Age$
Post. Lens (PL)	–6.86		
Post. Chamber (PC)		1.336	
Eye			$22.984 + 0.0113 \cdot Age$

The refractive index *n* of the lens was created using the GRIN power law equation [4]:

$$n = n_{\max} + (n_{\min} - n_{\max}) \cdot d^{2g} \tag{1}$$

where *n* is the index of refraction along the optic axis, and $n_{\max}$ is the maximum index at the lens center, $n_{\min}$ is the minimum refractive index at the lens surface, g is the power exponent and *d* is the normalized distance from the lens center (0), to the anterior lens surface (–1) and posterior lens surface (1) obtained by dividing by the respective distances along the optic axis for the respective age [4]. According to [4] $g = 2.5261$, $n_{\min} = 1.36$ and analysis of different $n_{\max}$ was made using fixed internal maximum index magnitudes: 1.41, 1.42, 1.43, 1.44, and an internal index that varies with age [4],

$$n_{\max}(Age) = 1.4385 - 0.0001 \cdot Age. \tag{2}$$

2.2 System matrix

To analyze the effects of the GRIN and the internal curvatures of the lens on the paraxial properties, the system matrix approach was used [24, 25]. The *ABCD* system matrix **M** of the eye model was constructed by multiplying refractive and transference matrices in reverse order to obtain

$$\mathbf{M} = \begin{pmatrix} A & B \\ C & D \end{pmatrix} = \mathbf{T}_{PC}\mathbf{L}\mathbf{T}_{AC}\mathbf{R}_{K2}\mathbf{T}_{K}\mathbf{R}_{K1}, \tag{3}$$

a 2×2 symplectic matrix where *B* is in units of length, *C* in units of inverse length, and *A,* and *D* are unitless. Subscripts are given in Table 1. Harris [24] describes *A* as the ametropia. When $A = 0$, the system is exit-plane focal, and in the case of an eye, it is emmetropic. **R** is the refractive matrix of the form

$$\mathbf{R} = \begin{pmatrix} 1 & 0 \\ (n_0 - n_1)/r & 1 \end{pmatrix} \tag{4}$$

Biomedical Optics EXPRESS

where n_0 and n_1 are the indices of refraction on the left and on the right of the refractive surface respectively, and r is the radius of curvature of the refractive surface. **T** is the transference matrix:

$$\mathbf{T} = \begin{pmatrix} 1 & t/n \\ 0 & 1 \end{pmatrix} \tag{5}$$

where t is the thickness or depth of the media (e.g. cornea, anterior, and posterior chamber), and n is the index of refraction of the medium.

Matrix **L** represents the lens and its GRIN structure, and is constructed from a succession of refractive and transference matrices, multiplied in reverse from the posterior to the anterior of the lens. According to Eq. (1) the lens is divided into a series of N shells which makes it possible to identify an index n for every i-th, and $(i+1)$-th shell, a thickness t of the i-th shell, and therefore the position of the shell within the eye model, as well as the radius of curvature r of the i-th shell.

In Fig. 1 the dioptric power of the eye model starts to approach stability when the number of shells exceeds 100 with a difference of 0.0037 D for 100 shells. To eliminate any variation, $N = 200$ was chosen for the eye model.

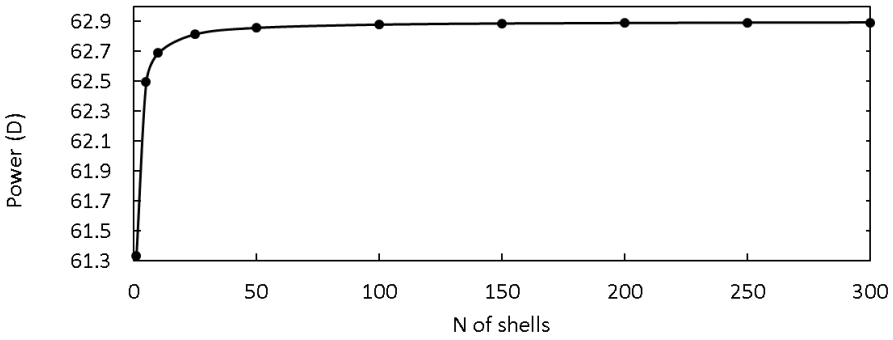

Fig. 1. Power of the eye model against the number of shells inside the lens (age 20 years).

A range of different models for the internal curvature were used, with power laws representing the index of refraction. For the i-th shell the radius is:

$$r_i = ad^p + bd^{p-1} + r_N \tag{6}$$

where p is the power of the polynomial equation, $a = -(r_{AL} + r_{PL})/2$, $b = (r_{AL} - r_{PL})/2 - r_N$. The subscripts and lens surface radii are given in Table 1. r_N is the radius of curvature of the nucleus of the lens, taken as positive. Directionality is observed, that is, r_{AL} is taken as positive and r_{PL} is taken as negative. Figure 2 shows the radii of the internal shells against the normalized distance d for four power laws using Eq. (6). For illustrative purposes, only the magnitudes of the radii of curvature are indicated. For power laws 3, 5, and 7 there is a flattened central section, indicating that the lens nucleus is equiconvex. The higher the power law, the greater the thickness of the lens nucleus. For power law 1, Eq. (6) becomes the equation for a straight line which does not provide a clear nucleus and, hence, differs significantly from the other power law curves.

Biomedical Optics EXPRESS

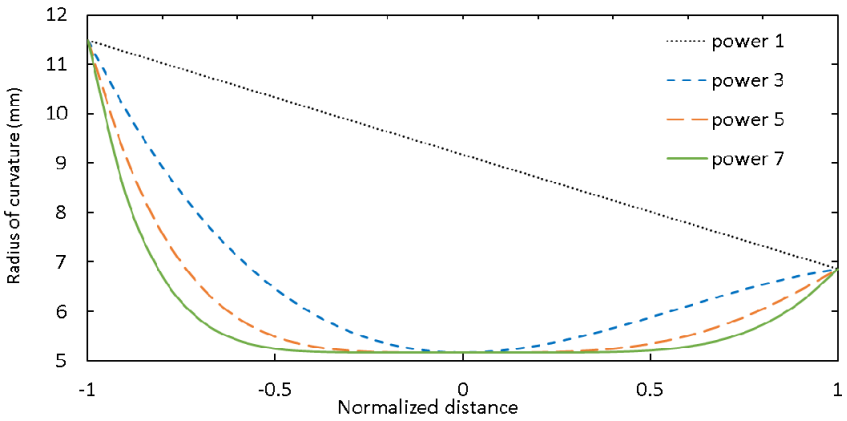

Fig. 2. Magnitudes of the radii of curvature of the internal shells of the lens against normalized distance *d*. Four different power laws (1, 3, 5, and 7) are presented. Parameters are based on an eye of age 20 years.

The internal nucleus of the lens is modelled to be a single entity i.e. homogenous refractive index and equiconvex, and therefore excludes power law 1. This adheres to previous studies that show a nucleus of uniform refractive index magnitude with no asymmetries between anterior and posterior contours [4, 26]. These empirical findings contrast with previous models such as the AVOCADO [23] or modified Navarro model [27] where the nucleus has different curvatures for its anterior and posterior surfaces. The power law is treated as unchanging with age.

To clarify the method used for the construction of matrix **L**, Fig. 3 shows the construction of the *i*-th shell. Each shell has the same index of refraction, however, whilst the lens nucleus is equiconvex, the radii for anterior and posterior profiles increase with progression towards the lens surface. This increase is greater for the anterior than for the posterior radii.

Biomedical Optics EXPRESS

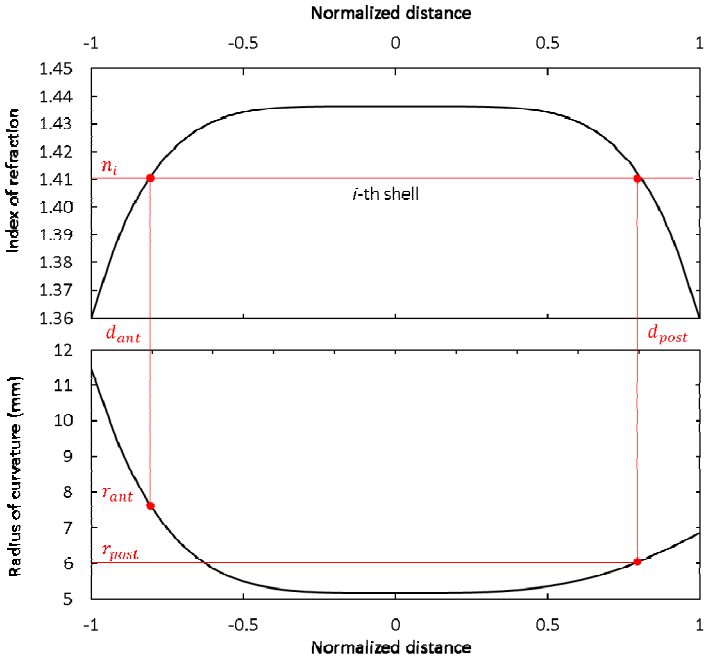

Fig. 3. The index of refraction n_i, position d inside the lens, and magnitude of the radii of curvature r_i for anterior and posterior part of the i-th shell for an eye of age 20 years and using power law 5.

Thus far, we have parameters for the eye as a function of age based on empirical data (Table 1) and relationships for the internal structure of the lens. Equation (1) gives us the refractive index and Eq. (6) gives us the radii of curvature for each shell. In the next section, we explore the effect of four power laws and five refractive indices for the lens nucleus $n_{\max}$ to obtain the combination that best compensates for the lens paradox with 200 shells.

Using MATLAB (MathWorks, Inc.) the GRIN profiles for the model eye for each of the four powers and five indices of refraction are derived and for each combination, we obtain the system matrix **M** and seek the r_N in each case that results in emmetropia, i.e. when $A = 0$ [24, 25], for the age range 20 to 70 years. The results are compared to the empirical GRIN profiles of the lenses [4, 26] and an optimal combination of r_N, $n_{\max}$ and power law suggested.

3. Results

Using a homogenous index of refraction for the lens and the age-related changes in the parameters given in Table 1, the change in power of the eye from age 20 to 70 years is around 1.63 D with a shift towards myopia. This is illustrated by the red line in Fig. 5. However, it is known from clinical experience that the eye does not become myopic with age, giving rise to the lens paradox.

According to the eye model and matrix optics described in the previous section and parameters given in Table 1, Fig. 4 shows the models for a 20 year old, 45 year old, and 70 year old lens, using power law 5 and $n_{\max}(Age)$ given by Eq. (2) for the index of the nucleus. Since we are not interested in wide-angle analysis, asphericity coefficients are not taken into account and all the surfaces in Fig. 4 are spherical. For the model presented as an example in Fig. 4 the system matrices are:

Biomedical Optics EXPRESS

$$\mathbf{M}_{20} = \begin{pmatrix} 0.0000 & 15.9008\times10^{-3}\ \text{m} \\ -62.8893\ \text{D} & 0.8976 \end{pmatrix} \tag{7}$$

$$\mathbf{M}_{45} = \begin{pmatrix} -0.0000 & 16.1410\times10^{-3}\ \text{m} \\ -61.9546\ \text{D} & 0.9022 \end{pmatrix} \tag{8}$$

$$\mathbf{M}_{70} = \begin{pmatrix} -0.0000 & 16.3908\times10^{-3}\ \text{m} \\ -61.0104\ \text{D} & 0.9074 \end{pmatrix} \tag{9}$$

where D (diopters) is m^{-1}. According to these matrices the power of the eye model changes with age, decreasing from 62.89 D at 20 years of age, to 61.95 D at 45 years of age, and 61.01 D at 70 years of age. The trend of power change with age is shown in Fig. 5 (solid black line). This is compared to the changing power of the eye with age using power law 1 and a nuclear refractive index $n_{\max} = 1.43$ (red dashed line).

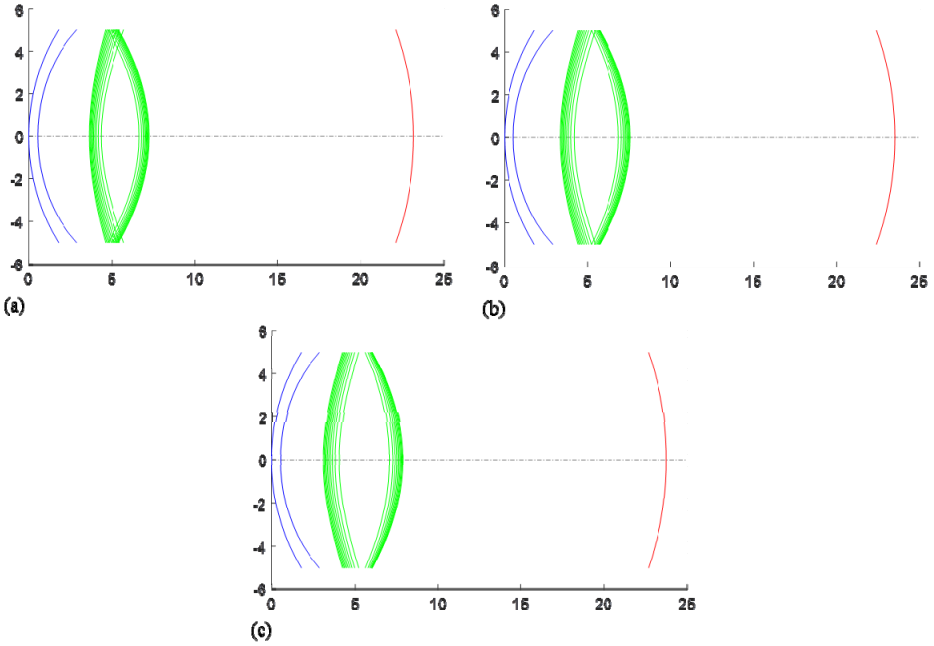

Fig. 4. Lens model of (a) 20 year old, (b) 45 year old, and (c) 70 year old, with lens nucleus of index of refraction $n_{\max}(Age)$ (Eq. (2) and power law 5. All measurements are in mm.

Biomedical Optics EXPRESS

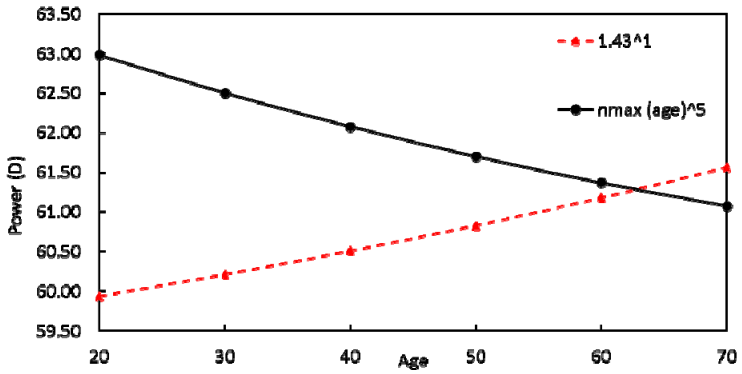

Fig. 5. Power of the eye model as a function of age according to parameters given in Table 1 and $n_{\max} = 1.43$. The red dashed line gives the power of the eye model with power law 1 and the black solid line to power law 5 and using $n_{\max}(Age)$.

The differences between models shown in Fig. 5 arise because of the contribution of different power laws and of differences in maximum refractive index. The red dashed line in Fig. 5, using power law 1 and a maximum refractive index $n_{\max} = 1.43$, does not satisfy the required power for maintaining emmetropia with age. However, using power law 5 and $n_{\max}(Age)$ (solid black line in Fig. 5) we are able to compensate for the lens paradox and the eye is emmetropic for ages 20 to 70 years. The system matrices **M** for the eye for ages 20, 45 and 70 years, given by Eqs. (7) to (9), all show that $A = 0$ i.e. they are all emmetropic.

In order to compensate for the changing power of the eye with age, as seen by the black line in Fig. 5, appropriate internal curvatures of the nucleus r_N were sought. With the application of different power laws, the nuclear radius of curvature was found to increase with age (Fig. 6). In young lenses in particular, the curvature of the nucleus is steeper compared to both anterior and posterior surfaces of the lens, indicating that the lens resembles an avocado [23]. With age this alters and in older lenses the nucleus is flatter than the posterior surface.

Biomedical Optics EXPRESS

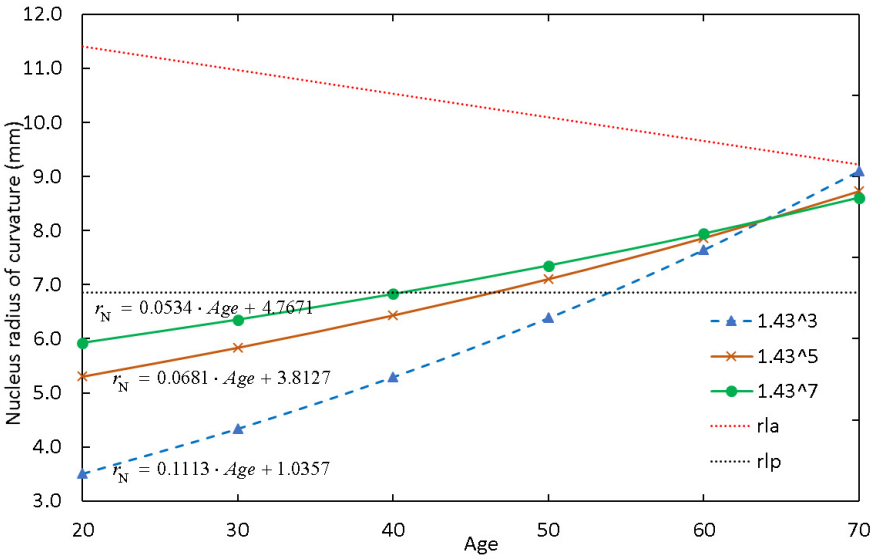

Fig. 6. Radius of curvature of the nucleus r_N as a function of age for different power laws. Radii of curvature of the anterior (rla - red dotted) and magnitude of the posterior (rlp - black dotted) lens surfaces are also given. The linear fits for r_N are given. The R^2 values are 0.9949, 0.9962 and 0.9968 for power laws 3, 5 and 7, respectively. $p < 0.001$ for all r_N fits.

Figure 6 shows the fits for the different power laws and indicates that as the power law increases, the slope of the line becomes flatter.

In order to analyze the effects of different nuclear indices of refraction, power law 5 was used to describe the internal GRIN structure of the lens. The relationships are given in Fig. 7.

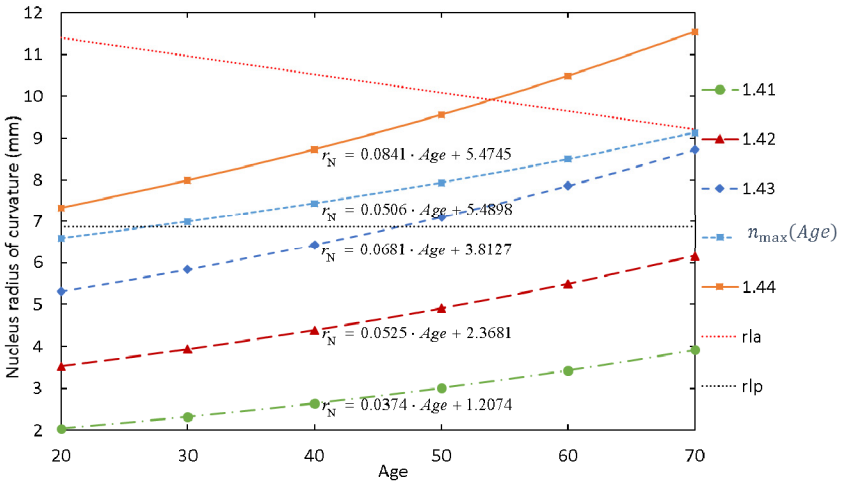

Fig. 7. Radius of curvature of the nucleus as a function of age for five different nuclear maximum index values using power law 5. The linear fits for r_N are given. Radii of curvature of the anterior (rla - red dotted) and magnitude of the posterior (rlp - black dotted) lens surfaces are also given. The R^2 values are 0.9951, 0,9957, 0.9962, 0.9965 and 0.9964 for n_{max} values of 1,41, 1.42, 1.43, $n_{max}(Age)$ and 1.44, respectively. $p < 0.001$ for all r_N fits.

Biomedical Optics EXPRESS

From Fig. 7 we see that the internal nuclear radius of curvature increases with age and with n_{max}. When comparing Figs. 6 and 7, it is apparent that the slope has a stronger dependence on the power law than on n_{max}.

Figure 7 shows the r_N as a function of age ranging from 20 to 70 years for a selection of five nuclear refractive indices using power law 5 and compares these to the anterior and posterior lens surface radii (Table 1). With the lowest values of n_{max} equal to 1.41 and 1.42, at every age r_N is steeper than both the anterior and posterior surfaces. When the value of n_{max} is equal to 1.43, the equator exhibits a steeper curvature compared to both anterior and posterior surfaces for younger people until the age of 45. After that, the curvature of the nucleus becomes flatter than the posterior surface. With $n_{max}(Age)$ according to Eq. (2) the equator is flatter than the posterior surface from age 27 but steeper than the anterior surface. With the highest refractive index value of 1.44, the nucleus is flatter than the posterior surface and becomes flatter than the anterior surface at the age of 53.

4. Discussion and conclusions

In order to investigate how the GRIN may offset changes in curvature with age and provide further insight into solving the lens paradox, an eye model based on experimental biometric data [19] was created. The *ABCD* system matrix [24, 25] formalism was used to obtain the r_N that results in emmetropia and, hence, addresses the lens paradox.

According to data for refractive index from in-vitro lenses [4, 26] and modelling the nucleus as a single entity rather than constructed from two halves, the curvatures of the nucleus were treated as equiconvex. This distinguishes the presented model from other models such as the AVOCADO [23] or the modified Navarro model [27].

This work shows the results of modelling the internal curvatures of the lens shells using four different power laws (i.e. 1, 3, 5, and 7) and, for every shell, a specific radius of curvature and index of refraction could be calculated for the normalized distance in the lens, constructing the system matrix **M** for the model eye. From Fig. 2 and Fig. 5 we saw that power law 1 follows a straight line profile for the change in radius of curvature and does not compensate for the lens paradox. For the GRIN profile chosen and for a fixed value of n_{max} with age, only a power law higher than 3 can counteract the increases in curvature with age in order to prevent myopia.

Changing the power law affects the nuclear central curvature with age. From Fig. 6 we see that the higher the power law, the flatter is the slope of the change of the nucleus curvature with age. Hence, with high power laws, the changes in nuclear curvature with age are minimal. Conversely, with low power laws the so-called avocado shape of the nucleus in younger lenses becomes evident.

The power law and the internal index of refraction of the nucleus n_{max} affect the shape of the lens. Choosing n_{max} equal to 1.41, 1.42, 1.43, 1.44 or $n_{max}(Age)$, an internal index that varies with age according to Pierscionek *et al* [4], we see from Fig. 7 that the nuclear internal curvature r_N becomes flatter with age. In particular, for low values of n_{max} that is 1.41 and 1.42, the nuclear curvature is always steeper than both external surfaces of the lens. With the mid-range values, that is 1.43 and $n_{max}(Age)$, the internal surface of the nucleus becomes flatter than the posterior surface of the lens and closely resembles empirical findings [4] for power laws 5 and 7. For 1.44 the internal surface of the lens nucleus is flatter than the posterior lens surface and after the age of 53, is also flatter than the anterior surface of the lens. The $n_{max}(Age)$ combined with power law 5 provides the closest resemblance to the empirical findings of Pierscionek *et al* [4].

Biomedical Optics EXPRESS

With age the anterior chamber depth decreases, the lens thickness and axial length increase, and the anterior radius of curvature of the lens becomes steeper [19]. According to the results of this work, the nucleus becomes flatter with age. The present study shows how the combination of a suitable nuclear refractive index with changes in internal curvatures of the lens may explain the lens paradox, and add to developing a better understanding of how the lens may alter with age. Alteration of the GRIN profile has been shown to offset a potential myopic shift resulting from curvature increase [28]. It should be noted that the lens is a biological structure and local alterations in refractive index, necessitating alterations in protein/water relationships [29], are likely to affect cell shape and hence curvature. Changes in refractive index with age can result from alterations in state of water that manifest in more protein bound water becoming free water [29,30] and can also occur in response to metabolic or glycation-like changes such as with hyperglycaemia as found in diabetic patients who have been shown to experience a hyperopic shift in response to elevated blood glucose [31]. Hyperopic shifts caused by alteration in refractive index were also observed as transient occurrences after initiating therapy for hyperglycaemia [32, 33] and in longer duration Type 2 diabetes [34]. It is further pertinent that lens surface shape varies in individuals and this can mask age-related changes. These individual variations and the biology that may underlie them requires further investigation in order to broaden the knowledge of optics of the eye and to advance the potential for personalized eye care.

Acknowledgment

We thank Prof. W.F. Harris for continuing discussions. BKP acknowledges funding from Fight for Sight grant no 1319/1320.